JVI Journals.ASM.org

Molecular Determinants of Virulence and Stability of a Reporter-Expressing H5N1 Influenza A Virus

Dongming Zhao,[a,b] Satoshi Fukuyama,[a,b] Shinya Yamada,[b] Tiago J. S. Lopes,[a] Tadashi Maemura,[b] Hiroaki Katsura,[b] Makoto Ozawa,[c,d] Shinji Watanabe,[a,e] Gabriele Neumann,[f] Yoshihiro Kawaoka[a,b,f,g]

Exploratory Research for Advanced Technology Infection-Induced Host Responses Project, Japan Science and Technology Agency, Saitama, Japan[a]; Division of Virology, Department of Microbiology and Immunology, Institute of Medical Science, University of Tokyo, Shirokanedai, Tokyo, Japan[b]; Laboratory of Animal Hygiene, Joint Faculty of Veterinary Medicine, Kagoshima University, Kagoshima, Japan[c]; Transboundary Animal Distance Center, Joint Faculty of Veterinary Medicine, Kagoshima University, Kagoshima, Japan[d]; Microbiology, Department of Veterinary Sciences, University of Miyazaki, Miyazaki, Japan[e]; Department of Pathobiological Sciences, School of Veterinary Medicine, University of Wisconsin—Madison, Madison, Wisconsin, USA[f]; Department of Special Pathogens, International Research Center for Infectious Diseases, Institute of Medical Science, University of Tokyo, Tokyo, Japan[g]

ABSTRACT

We previously reported that an H5N1 virus carrying the Venus reporter gene, which was inserted into the NS gene segment from the A/Puerto Rico/8/1934(H1N1) virus (Venus-H5N1 virus), became more lethal to mice, and the reporter gene was stably maintained after mouse adaptation compared with the wild-type Venus-H5N1 (WT-Venus-H5N1) virus. However, the basis for this difference in virulence and Venus stability was unclear. Here, we investigated the molecular determinants behind this virulence and reporter stability by comparing WT-Venus-H5N1 virus with a mouse-adapted Venus-H5N1 (MA-Venus-H5N1) virus. To determine the genetic basis for these differences, we used reverse genetics to generate a series of reassortants of these two viruses. We found that reassortants with PB2 from MA-Venus-H5N1 (MA-PB2), MA-PA, or MA-NS expressed Venus more stably than did WT-Venus-H5N1 virus. We also found that a single mutation in PB2 (V25A) or in PA (R443K) increased the virulence of the WT-Venus-H5N1 virus in mice and that the presence of both of these mutations substantially enhanced the pathogenicity of the virus. Our results suggest roles for PB2 and PA in the stable maintenance of a foreign protein as an NS1 fusion protein in influenza A virus.

IMPORTANCE

The ability to visualize influenza viruses has far-reaching benefits in influenza virus research. Previously, we reported that an H5N1 virus bearing the Venus reporter gene became more pathogenic to mice and that its reporter gene was more highly expressed and more stably maintained after mouse adaptation. Here, we investigated the molecular determinants behind this enhanced virulence and reporter stability. We found that mutations in PB2 (V25A) and PA (R443K) play crucial roles in the stable maintenance of a foreign protein as an NS1 fusion protein in influenza A virus and in the virulence of influenza virus in mice. Our findings further our knowledge of the pathogenicity of influenza virus in mammals and will help advance influenza virus-related live-imaging studies *in vitro* and *in vivo*.

Highly pathogenic avian influenza viruses (HPAIVs) of the H5N1 subtype continue to evolve in nature, threatening animal and public health. These viruses were first identified in Guangdong province in China in 1996 (1) and have since been found in over 63 countries in multiple avian species, repeatedly infecting mammals such as pigs and humans (2, 3). By January 2015, 694 human cases of H5N1 virus infection had been confirmed by the World Health Organization (WHO), 402 of which were fatal, yielding a case fatality rate of almost 60% (http://www.who.int/). In addition, novel subtypes of influenza viruses, such as H7N9 and H10N8, have emerged and sporadically infected humans, causing fatal outcomes (4, 5) (http://www.who.int/). Thus, the constant threat from influenza viruses reminds us of the urgent need to gain a thorough understanding of their pathogenic mechanism in order to develop more effective strategies for control.

Although influenza virus has been extensively studied, many fundamental issues associated with the dynamic processes of influenza virus infection and virus target cells *in vivo* remain inadequately understood. The ability to visualize influenza viruses expressing a fluorescent reporter gene will shed new light on these issues (6, 7). By following a previously reported strategy (7), we successfully constructed an H5N1 virus with the Venus (a variant of enhanced green fluorescent protein [eGFP] [8]) reporter gene (designated wild-type Venus-H5N1 [WT-Venus-H5N1] virus) by using reverse genetics; this virus showed moderate virulence and low Venus expression levels in mice (9). After six passages in mice, we acquired a mouse-adapted Venus-H5N1 (MA-Venus-H5N1) virus that stably expressed high levels of Venus *in vivo* and was lethal to mice; the dose required to kill 50% of infected mice (50% minimum lethal dose [MLD_{50}]) was 3.2 PFU, whereas that of its parent WT-Venus-H5N1 virus was 10^3 PFU. However, the mo-

Received 30 July 2015 **Accepted** 24 August 2015

Accepted manuscript posted online 2 September 2015

Citation Zhao D, Fukuyama S, Yamada S, Lopes TJS, Maemura T, Katsura H, Ozawa M, Watanabe S, Neumann G, Kawaoka Y. 2015. Molecular determinants of virulence and stability of a reporter-expressing H5N1 influenza A virus. J Virol 89:11337–11346. doi:10.1128/JVI.01886-15.

Editor: T. S. Dermody

Address correspondence to Yoshihiro Kawaoka, kawaoka@ims.u-tokyo.ac.jp.

lecular determinants for this difference in virulence and Venus stability were unclear.

In this study, we explored the molecular determinants for the virulence and Venus stability of Venus-H5N1 virus in mice. By using reverse genetics, we rescued various reassortants between the WT-Venus-H5N1 and MA-Venus-H5N1 viruses. We then examined their virulence in mice to identify determinants for pathogenicity. Furthermore, we investigated the determinants for Venus expression and Venus stability *in vitro* and *in vivo*. Our findings advance our understanding of the pathogenicity of influenza virus in mammals and will benefit influenza virus-related live-imaging studies *in vitro* and *in vivo*.

MATERIALS AND METHODS

Cells. Human embryonic kidney HEK 293 and HEK 293T cells were maintained in Dulbecco's modified Eagle's medium (DMEM) with 10% fetal calf serum, and Madin-Darby canine kidney (MDCK) cells were maintained in minimal essential medium (MEM) supplemented with 5% newborn calf serum. All cells were incubated at 37°C in 5% CO_2.

Plasmid construction. Plasmids for virus rescue were constructed as described previously (9, 10). To measure viral polymerase activity, the open reading frames of the PB1, PB2, PA, and NP genes of influenza virus were amplified by PCR with gene-specific primers and cloned into the pCAGGS/MCS protein expression plasmid (11, 12). The primer sequences are available upon request. All of the constructs were completely sequenced to ensure the absence of unwanted mutations.

Plasmid-based reverse genetics. Influenza A viruses were generated by using plasmid-based reverse genetics, as described previously (10). Viral titers of the rescued viruses were determined by use of plaque assays in MDCK cells. All rescued viruses were sequenced to confirm the absence of unwanted mutations.

Mouse experiments. Six-week-old female C57BL/6 mice (Japan SLC, Inc., Shizuoka, Japan) were used in this study. To measure viral replication in mice, six mice in each group were anesthetized with isoflurane and then intranasally inoculated with 10^5 PFU (50 μl) of virus. On days 1 and 3 postinfection (p.i.), three mice were euthanized, and their organs, including the lungs, kidneys, spleens, and brains, were collected and titrated in MDCK cells. To determine the MLD_{50} values of the viruses, four mice from each group were inoculated intranasally with 10-fold serial dilutions containing 10^0 to 10^5 PFU (50 μl) of virus. Body weight and survival were monitored daily for 14 days. MLD_{50} values were calculated by using the method of Reed and Muench (13). All mouse experiments were performed in accordance with the University of Tokyo's Regulations for Animal Care and Use and were approved by the Animal Experiment Committee of the Institute of Medical Science, University of Tokyo.

Virus passage in mice and MDCK cells. Mouse adaptation of virus was performed as described previously (9). For virus passages in MDCK cells, confluent MDCK cells were infected with virus at a multiplicity of infection (MOI) of 0.0001. At 48 h postinfection (hpi), the supernatants were collected and titrated in MDCK cells. The new, harvested viruses were used to infect MDCK cells for the next passage. This procedure was repeated five times.

Quantification of Venus expression by use of flow cytometry. MDCK cells were infected with virus at an MOI of 0.001. At 24 hpi, the cells were digested with trypsin to obtain a single-cell suspension. Data were acquired on a FACSAria II instrument (BD Biosciences), and the mean fluorescence intensity (MFI) was analyzed with FlowJo X 10.0.7r2 software (Tree Star, San Carlos, CA).

Growth kinetics assays. Each virus was inoculated into triplicate wells of subconfluent MDCK cells at an MOI of 0.0001. The cells were supplemented with MEM containing 0.3% bovine serum albumin (BSA) and 1 μg/ml tosylsulfonyl phenylalanyl chloromethyl ketone (TPCK) trypsin and incubated at 37°C in 5% CO_2. Culture supernatants were harvested at the indicated times postinfection. The viral titers of the supernatants at different time points were determined by use of plaque assays in MDCK cells.

Minigenome luciferase assay. Polymerase activity was tested with a minigenome assay by using the dual-luciferase system, as previously described (14, 15). Briefly, HEK 293 cells were transfected with viral protein expression plasmids for NP, PB1, PB2, and PA from the WT-Venus-H5N1 or MA-Venus-H5N1 virus (0.2 μg each); a plasmid expressing a reporter viral RNA (vRNA) encoding the firefly luciferase gene under the control of the human RNA polymerase I promoter [pPolI/NP(0)Fluc(0); 0.2 μg]; and pRL-null (0.2 μg; Promega), which encodes *Renilla* luciferase, as an internal transfection control. At 24 h posttransfection, the cell lysate was prepared with the Dual-Luciferase Reporter assay system (Promega), and luciferase activity was measured by using the GloMax 96 microplate luminometer (Promega). The assay was standardized against *Renilla* luciferase activity. All experiments were performed in triplicate.

Western blotting. Mouse monoclonal antibodies against PB2 (18/1), PB1 (136/1), and PA (65/4) were available in our laboratory, and the mouse antibody against β-actin (clone AC-74) was purchased from Sigma-Aldrich. Enhanced chemiluminescence (ECL) anti-mouse IgG horseradish peroxidase-linked whole antibody (from sheep) was purchased from GE Healthcare. Western blotting was performed as described previously (16). Briefly, the samples were lysed with 2× SDS loading buffer (Invitrogen) and subjected to SDS-polyacrylamide gel electrophoresis (SDS-PAGE). Proteins on SDS-PAGE gels were transferred electrophoretically to a polyvinylidene difluoride (PVDF) membrane (Millipore). The membrane was blocked with Blocking One (Nacalai Tesque) for 30 min and was then incubated with the primary antibodies for 3 h at room temperature, followed by three washes with phosphate-buffered saline (PBS) plus Tween 20 (PBS-T). The membrane was incubated with the secondary antibody for 1 h at room temperature and washed three times with PBS-T. The membrane was then incubated with SuperSignal West Femto Maximum Sensitivity substrate (Thermo Scientific Pierce). Specific proteins were detected and quantified with the VersaDoc imaging system (Bio-Rad).

Laboratory facility. All studies with H5N1 viruses were performed in enhanced biosafety level 3 containment laboratories at the University of Tokyo (Tokyo, Japan), which are approved for such use by the Ministry of Agriculture, Forestry, and Fisheries of Japan.

Statistical analysis. The data were analyzed by using R software, version 3.1 (http://www.r-project.org/). For comparisons of measurements from multiple groups collected at a single time point, we used one-way analysis of variance (ANOVA) followed by Tukey's *post hoc* test (see Fig. 6A). For comparisons of multiple groups with measurements collected independently at different time points (i.e., viral growth curves from mice, collected in MDCK cells [Table 1]), we used two-way ANOVA followed by Tukey's *post hoc* test. For comparisons of multiple groups with dependent measurements (i.e., viral growth curves in cell culture for which aliquots were collected from the same culture at different time points [see Fig. 5]), we fitted a linear mixed-effects model to the data using the R package NLME, and the time, the virus strain, and interaction between these two factors were considered. Next, we built a contrast matrix to compare the strains in a pairwise fashion at the same time points (e.g., group 1 versus group 2 at 24 h postinfection, group 1 versus group 3 at 24 h postinfection, and group 2 versus group 3 at 24 h postinfection), using the R package PHIA. Because the comparisons were performed individually, the final *P* values were adjusted by using Holm's method to account for multiple comparisons (49).

In all cases, the results were considered statistically significant if we obtained *P* values (or adjusted *P* values) of <0.05.

Sequence analysis. The PB2 and PA sequences from the Influenza Research Database (http://www.fludb.org/) were aligned by using the MUSCLE program (17), with the default parameters and a maximum of 100 iterations. The alignment was visualized by using Clustal X (18), and the frequency of amino acid occurrences at specific positions was determined by using custom-written Perl scripts.

TABLE 1 Replication and virulence of H5N1 reassortants and mutants in mice[a]

Virus	Mean virus titer (log_{10} PFU/g) ± SD[b]							
	Lung		Spleen		Kidney		Brain	
	Day 1 p.i.	Day 3 p.i.	Day 1 p.i.	Day 3 p.i.	Day 1 p.i.	Day 3 p.i.	Day 1 p.i.	Day 3 p.i.
WT-Venus-H5N1	6.5 ± 0.2	6.3 ± 0.2	—	—	—	—	—	—
MA-Venus-H5N1[d]	9.1 ± 0.1[c]	8.9 ± 0.0[c]	3.4 ± 0.2	6.5 ± 0.1	2.4 ± 0.1	4.1 ± 0.1	—	2.8 ± 0.6
rgMA-Venus-H5N1	9.1 ± 0.1[c]	9.2 ± 0.1[c]	2.8 ± 0.4	7.1 ± 0.0	2.3, —, —	4.0 ± 0.1	—	2.3 ± 0.2
WT+MA-PB2	7.7 ± 0.0[c]	8.0 ± 0.1[c]	—	4.1, 4.4, —	—	—	—	—
WT+MA-PA	7.1 ± 0.1[c]	6.8 ± 0.1[c]	—	—	—	—	—	—
WT+MA-(PB2+PA)	8.6 ± 0.3[c]	8.7 ± 0.1[c]	2.9 ± 0.4	6.8 ± 0.0	2.0, 1.7, —	4.3 ± 0.7	—	2.7 ± 0.8
VN1203	8.6 ± 0.1	8.5 ± 0.1	2.9, 2.9, —	6.4 ± 0.4	1.8, 2.1, —	4.0 ± 0.8	—	2.9 ± 0.6

[a] Six-week-old specific-pathogen-free C57BL/6 mice were inoculated intranasally with 10^5 PFU of each virus in a 50-μl volume. Three mice from each group were euthanized on days 1 and 3 p.i., and virus titers in samples of lung, spleen, kidney, and brain were determined in MDCK cells.
[b] —, no virus was isolated from the sample.
[c] The *P* value was <0.05 compared with the titers in the lungs of mice infected with WT-Venus-H5N1 virus.
[d] Viral titers for MA-Venus-H5N1 virus on day 3 p.i. were reported previously (9).

RESULTS

Comparison between WT-Venus-H5N1 and MA-Venus-H5N1 viruses. Previously, we replaced the NS segment of A/Viet Nam/1203/2004(H5N1) (VN1203) with a Venus-fused NS segment of Venus-A/Puerto Rico/8/1934(H1N1) (PR8) virus by using reverse genetics and acquired an H5N1 virus that expressed the Venus fluorescent reporter gene (WT-Venus-H5N1 virus) (9). A pathogenicity analysis in mice revealed that the virulence of this virus was attenuated (with an MLD_{50} value of 10^3 PFU) (Fig. 1) compared with that of the parental VN1203 virus (MLD_{50}, 3.2 PFU) (Fig. 1) (19). Moreover, WT-Venus-H5N1 virus replicated only in respiratory organs (Table 1), and its Venus expression was very weak in both MDCK cells (Fig. 2) and mice after virus infection (Fig. 3).

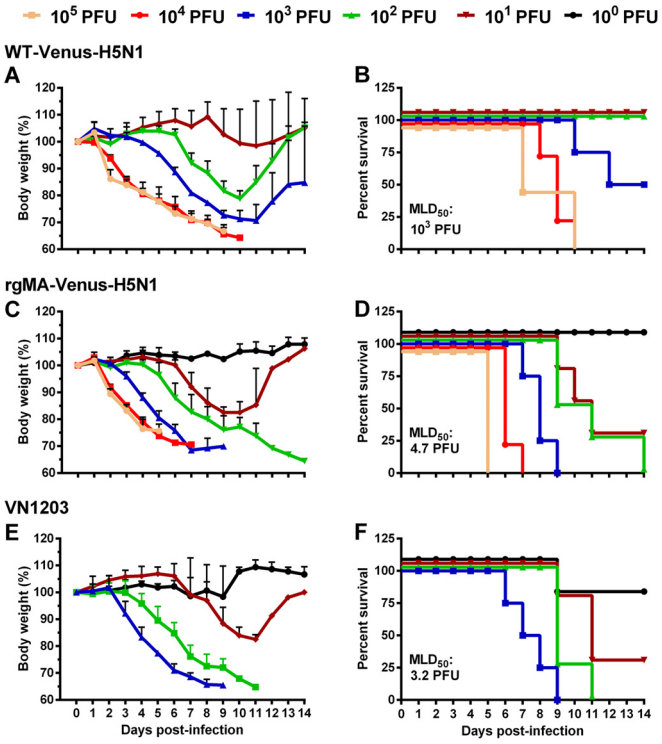

FIG 1 Virulence of WT-Venus-H5N1 virus and rgMA-Venus-H5N1 virus in mice. Groups of four mice were intranasally infected with 10^0 to 10^5 PFU of WT-Venus-H5N1 virus, rgMA-Venus-H5N1 virus, or VN1203 virus. Body weight changes (A, C, and E) and survival (B, D, and F) were monitored for 2 weeks.

After six passages of WT-Venus-H5N1 virus in mice, MA-Venus-H5N1 virus was obtained. MA-Venus-H5N1 virus was lethal to mice, with an MLD_{50} of 3.2 PFU, which was the same as that of the parental VN1203 virus (Fig. 1E and F) (9, 19). This virus replicated systemically in mice, comparably to the parental VN1203 virus; on day 1 p.i., high viral titers were detected in the lungs, spleens, and kidneys, and on day 3 p.i., virus was detected in the brain (Table 1) (note that viral titers for MA-Venus-H5N1 virus on day 3 p.i. were reported previously [9]). Moreover, we detected high Venus expression levels for MA-Venus-H5N1 virus in MDCK cells (Fig. 2) and in mice (Fig. 3). These results demonstrate that, compared with WT-Venus-H5N1, MA-Venus-H5N1 virus has high pathogenicity in mice and a high replicative ability. Moreover, this virus exhibited high Venus expression levels during its replication *in vitro* and *in vivo*.

To identify the mutations that occurred during mouse adaptation, we performed Sanger sequencing of reverse transcriptase PCR (RT-PCR) products derived from viral genes and compared them with those of WT-Venus-H5N1 virus. We found a total of seven differences between the two viruses in their PB1, PB2, PA, NA, M2, and NS1 proteins (Table 2). In addition, three silent mutations were identified: T558C and A741G in the NP gene and C1052T in the NA gene.

The V25A mutation in PB2 and the R443K mutation in PA determine the pathogenicity and Venus expression of Venus-H5N1 virus in mice. To investigate the genetic basis for the difference in the virulence and Venus expression of Venus-H5N1 virus after mouse adaptation, we established a reverse-genetics system for MA-Venus-H5N1 virus, which we named rgMA-Venus-H5N1 virus. This virus exhibited characteristics similar to those of MA-Venus-H5N1 virus with respect to viral titers in organs (Table 1), MLD_{50} values (Fig. 1C and D and 4), and Venus expression in mice (Fig. 3).

To identify the amino acids responsible for the difference in virulence and Venus expression between WT-Venus-H5N1 and MA-Venus-H5N1 viruses, we generated six single-gene reassortant viruses, each bearing the PB2, PB1, PA, NA, M, or NS gene from MA-Venus-H5N1 virus and the other seven genes from WT-

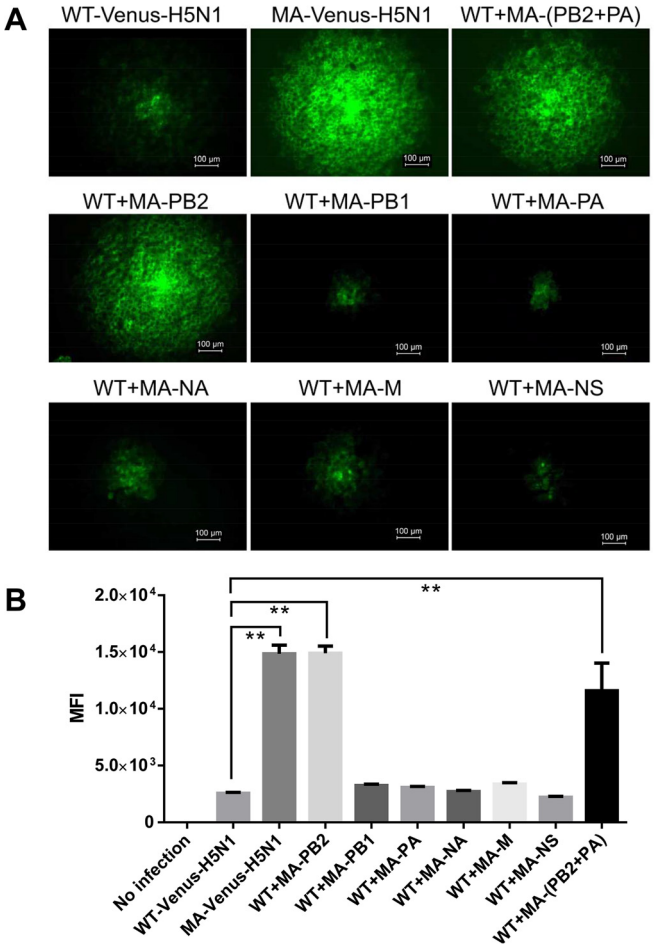

FIG 2 Venus expression of various H5N1 viruses in MDCK cells. (A) MDCK cells were infected with Venus-H5N1-related viruses, and at 24 hpi, the Venus expression of each virus plaque was observed by using fluorescence microscopy (Axio Observer.Z1; Zeiss). A representative image of each virus is shown. (B) MDCK cells were infected with Venus-H5N1-related viruses at an MOI of 0.001, and at 24 hpi, MDCK cells were digested with trypsin into single cells and analyzed by flow cytometry. The mean fluorescence intensity (MFI) was calculated by using FlowJo X 10.0.7r2. The values are means ± standard deviations from two independent experiments. **, $P < 0.01$ compared with WT-Venus-H5N1 virus-infected cells.

Venus-H5N1 virus. The recombinant viruses that contained the PB1, NA, or NS gene of MA-Venus-H5N1 virus (designated WT+MA-PB1, WT+MA-NA, and WT+MA-NS, respectively) displayed pathogenicity in mice similar to that of WT-Venus-H5N1 (MLD_{50}, 10^3 PFU) (Fig. 4), whereas the reassortants with the PB2, PA, or M gene of MA-Venus-H5N1 (designated WT+MA-PB2, WT+MA-PA, and WT+MA-M, respectively) exhibited higher pathogenicity in mice than did WT-Venus-H5N1 (Fig. 4). WT+MA-PB2 and WT+MA-PA also replicated more efficiently in mouse lungs than did WT-Venus-H5N1; moreover, virus was detected in the spleens of two of three mice infected with WT+MA-PB2 (Table 1).

The effect of the PB2, PA, or M gene derived from WT-Venus-H5N1 on the virulence of MA-Venus-H5N1 was also examined by generating three single-gene recombinant viruses, each containing the PB2, PA, or M gene from WT-Venus-H5N1 virus and the remaining segments from MA-Venus-H5N1 virus (designated MA+WT-PB2, MA+WT-PA, and MA+WT-M, respectively). The MLD_{50} values of MA+WT-PB2 and MA+WT-PA were $10^{2.3}$ PFU, which is significantly higher than that of rgMA-Venus-H5N1 (MLD_{50}, 4.7 PFU), whereas the virulence of MA+WT-M in mice was similar to that of rgMA-Venus-H5N1 (Fig. 4). These data suggest that the PB2 and PA genes play an important role in the pathogenicity of MA-Venus-H5N1 virus in mice.

To assess the potential for synergistic effects of the PB2 and PA genes on viral pathogenicity in mice, we rescued a reassortant carrying both the PB2 and PA genes of MA-Venus-H5N1 [MA-(PB2+PA)] on the WT-Venus-H5N1 virus backbone and the reciprocal reassortant on the MA-Venus-H5N1 virus backbone [designated WT+MA-(PB2+PA) and MA+WT-(PB2+PA), respectively] and assessed their virulence in mice. Substitution of the PB2 and PA genes from MA-Venus-H5N1 virus in WT-Venus-H5N1 virus significantly enhanced its virulence in mice, with an MLD_{50} value of 3.2 PFU (Fig. 4), and also enhanced virus spread and replication in mice (Table 1), similar to that of MA-Venus-H5N1 virus. Similarly, substitution of the PB2 and PA genes from WT-Venus-H5N1 virus in MA-Venus-H5N1 virus substantially attenuated its pathogenicity in mice (MLD_{50} value of $10^{3.0}$ PFU) (Fig. 4). Given that a single mutation is present in PB2 and in PA after mouse adaptation, these data indicate that the V25A mutation in PB2 and the R443K mutation in PA synergistically contribute to the virulence of MA-Venus-H5N1 virus in mice.

When we examined the Venus expression of the above-described reassortants in MDCK cells, we found that the MA-PB2 gene markedly increased Venus expression (Fig. 2A). Flow cytometry analysis also revealed that MA-PB2 contributed significantly to the high intensity of Venus expression in MDCK cells (Fig. 2B). In addition, Venus expression of WT+MA-PB2 virus in the lungs of mice was also appreciably enhanced (Fig. 3). The other single-gene substitutions, including MA-PA, did not affect Venus expression; however, the double substitution of MA-PB2 and MA-PA on the WT-Venus-H5N1 virus backbone increased Venus expression in mouse lung compared with those achieved by WT-Venus-H5N1 and WT+MA-PB2 viruses (Fig. 3). These data indicate that the V25A mutation in PB2 plays a vital role in the Venus expression of MA-Venus-H5N1 virus *in vitro* and *in vivo* and that the R443K mutation in PA enhances the PB2 effect on Venus expression.

The amino acid at position 25 in the PB2 protein significantly enhances viral replication in mammalian cells. We further examined the replicative ability of these viruses in MDCK cells and found that MA-Venus-H5N1 virus had a replicative capability similar to that of rgMA-Venus-H5N1 virus, with both viruses growing more efficiently than WT-Venus-H5N1 virus, and that the titers of MA-Venus-H5N1 virus were significantly higher than those of WT-Venus-H5N1 virus at 36 and 48 hpi (Fig. 5). We then investigated the contribution of the PB2 and PA gene segments to the replication of these two viruses. We observed significantly higher titers of WT+MA-PB2 and WT+MA-(PB2+PA) than those of WT-Venus-H5N1 virus at several time points postinfection, yet the replication efficiency of WT+MA-PA was comparable to that of WT-Venus-H5N1 virus (Fig. 5). At 36 and 48 hpi, the titers of WT+MA-(PB2+PA) were higher than those of WT+MA-PB2, although this difference was not statistically significant (Fig. 5). These results indicate that the MA-PB2 gene enhances the replication of Venus-H5N1 virus in MDCK cells and that this increase can be further enhanced by the presence of MA-

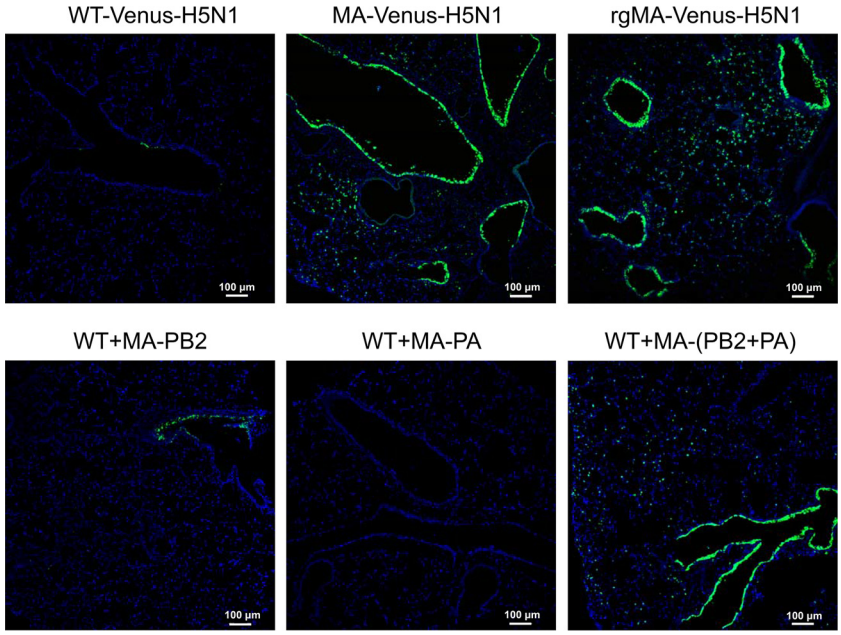

FIG 3 Venus expression of various H5N1 viruses in mouse lung. Groups of three mice were intranasally infected with 10^5 PFU (50 μl) of virus. The mice were euthanized on day 2 p.i., and their lungs were collected, fixed in 4% paraformaldehyde, and then embedded in OCT compound. The frozen tissues were cut into 5-μm slices and then stained with Hoechst 33342 dye. Venus signal was detected by using the Nikon A1$^+$ confocal microscope system. Blue represents nuclei stained with Hoechst 33342 dye; green represents Venus expression.

PA, although MA-PA alone does not alter virus replication in MDCK cells.

Mutations in the polymerase genes after mouse adaptation decrease viral polymerase activity in mammalian cells. The polymerase activity of the viral ribonucleoprotein (RNP) complex has been correlated with viral replication and virulence (20–23). The activity of the eight RNP combinations of PB1, PB2, and PA from either WT-Venus-H5N1 or MA-Venus-H5N1 virus was determined by measuring luciferase activity. The polymerase activity of the mouse-adapted virus was nearly 4-fold lower than that of WT-Venus-H5N1 virus (Fig. 6A). Substitution of any MA gene decreased the activity of the polymerase complex of WT-Venus-H5N1 virus, but the polymerase activity of complexes containing the double substitution of MA-PB2 and MA-PA was significantly decreased compared with that of WT-Venus-H5N1 virus and was similar to that of MA-Venus-H5N1 virus. We compared the expression levels of polymerase proteins by means of Western blot analysis and found that the mutations in PB2, PB1, and PA did not affect their expression levels (Fig. 6B), suggesting that the decrease in polymerase activity was not caused by changes in polymerase protein expression levels. These results indicate that the polymerase activity of the RNP complexes was notably decreased after mouse adaptation, which is not consistent with the enhanced replication and virulence observed.

Molecular determinants of Venus stability in Venus-H5N1 virus *in vitro* and *in vivo*. To assess Venus stability in the WT-Venus-H5N1 and rgMA-Venus-H5N1 viruses *in vitro*, we passaged the two viruses five times in MDCK cells. During these pas-

TABLE 2 Amino acid differences between WT-Venus-H5N1 and MA-Venus-H5N1 viruses

Viral protein	Amino acid position	Amino acid in:	
		WT-Venus-H5N1	MA-Venus-H5N1
PB2	25	Val	Ala
PB1	737	Lys	Arg
PA	443	Arg	Lys
NA	35	Ser	Arg
	284	Val	Leu
M2	64	Ala	Asp
NS1	167	Pro	Ser

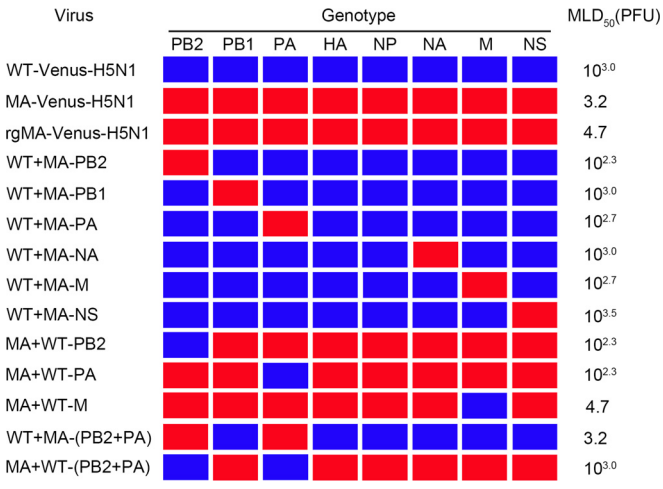

FIG 4 Genotypes of Venus-H5N1-related reassortants and their virulence in mice. The colors indicate the origins of the gene segments (blue, WT-Venus-H5N1 virus; red, MA-Venus-H5N1 virus). MLD_{50} values were determined by inoculating groups of four mice with 10-fold serial dilutions containing 10^0 to 10^5 PFU of virus in a 50-μl volume and were calculated by using the method of Reed and Muench (13).

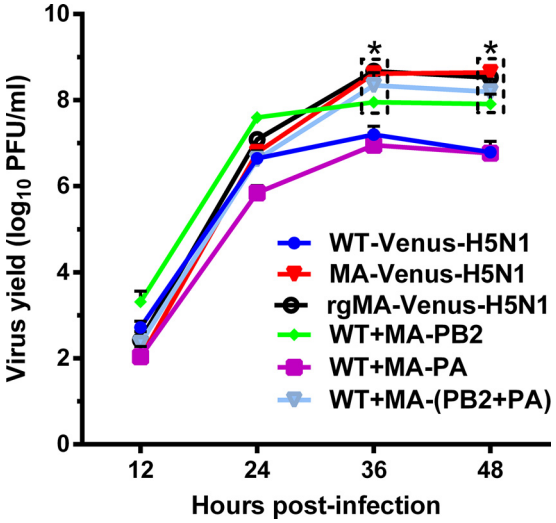

FIG 5 Growth kinetics of reassortants in MDCK cells. MDCK cells were infected with virus at an MOI of 0.0001, and culture supernatants were collected at the indicated times and then titrated in MDCK cells. The reported values are means ± standard deviations from two independent experiments. *, $P < 0.05$ compared with WT-Venus-H5N1 virus-infected cells.

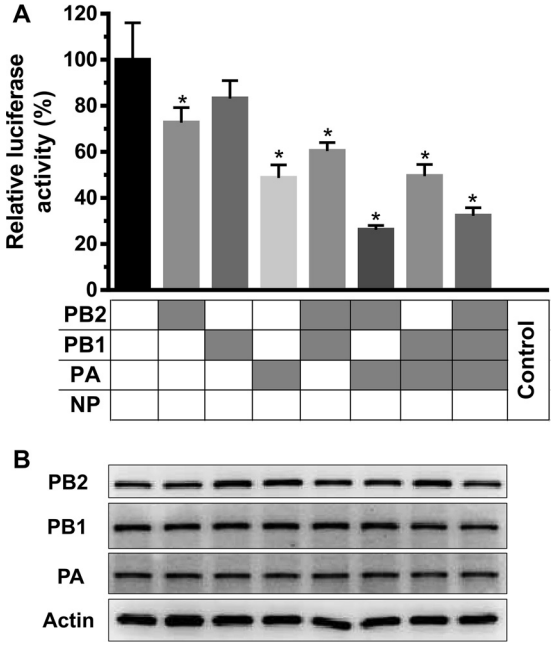

FIG 6 Polymerase activity and polymerase gene expression of different RNP combinations derived from the WT-Venus-H5N1 and MA-Venus-H5N1 viruses. HEK 293 cells were transfected in triplicate with a luciferase reporter plasmid and an internal control plasmid, together with plasmids expressing PB1, PB2, PA, and NP from either WT-Venus-H5N1 or MA-Venus-H5N1 virus. Segments derived from WT-Venus-H5N1 virus are shown in white, whereas those derived from MA-Venus-H5N1 virus are shown in gray. (A) Cells were incubated at 37°C for 24 h, and cell lysates were analyzed for firefly and *Renilla* luciferase activities. The values shown are means ± standard deviations of data from three independent experiments and are standardized to the activity of WT-Venus-H5N1 (100%). *, $P < 0.05$ compared with WT-Venus-H5N1 virus. (B) Plasmid-transfected cells were homogenized in 2× SDS loading buffer and then analyzed by Western blotting to measure the expression levels of PB2, PB1, and PA. Representative images are from three independent experiments.

sages, we found Venus-negative plaques from WT-Venus-H5N1 virus but not from rgMA-Venus-H5N1 virus, suggesting that the Venus gene is more stable after mouse adaptation (Table 3). To identify the molecular determinants of this Venus stability, various reassortants were passaged five times in MDCK cells. We obtained Venus-negative plaques from reassortants with the MA-PB1, MA-NA, or MA-M gene but not from Venus-H5N1 virus with the MA-PB2, MA-PA, MA-(PB2+PA), or MA-NS gene (Table 3). These data suggest that the MA-PB2, -PA, and -NS genes play a role in Venus stability.

To further evaluate the role of these different genes in Venus stability, the NS segments of the fifth-passage stocks from different reassortants were amplified by using RT-PCR and NS-specific primers. In addition to the Venus-NS segment (1.9 kb), the deleted NS segments were detectable. The bands corresponding to the deleted NS segments of WT-Venus-H5N1 and of the reassortants with the MA-NA and MA-M genes were much more intense than were those of the other reassortants (Fig. 7), further implying that the MA-NA and MA-M genes do not contribute to Venus stability *in vitro* and suggesting that reassortants with MA-NS, MA-PA, MA-PB2, or MA-PB1 may stably maintain the Venus-NS segment. Although rgMA-Venus-H5N1 virus and the reassortants with MA-NS, MA-PA, MA-PB2, or MA-PB1 were more stable, the deleted Venus-NS segments were still detectable by RT-PCR albeit to a lesser degree (Fig. 7). The deleted NS segments from the various reassortants were extracted and sequenced, and the different deletion forms were identified from the different reassortants (Fig. 8). The discrepancy between the results of RT-PCR and those of the plaque assays was likely due to assay sensitivity.

In addition, to examine Venus stability *in vivo*, we also inoculated C57BL/6 mice with 10^5 PFU of WT-Venus-H5N1 virus, rgMA-Venus-H5N1 virus, or WT+MA-(PB2+PA) virus. Lungs were collected on day 4 p.i. and were homogenized in PBS. The supernatants were inoculated into MDCK cells, and at 48 hpi, Venus-negative plaques were picked up and amplified in MDCK cells. We examined >95 plaques from each lung and found only 1 plaque without Venus expression from one of three mice infected with rgMA-Venus-H5N1 virus, 12 Venus-negative plaques from three mice infected with WT+MA-(PB2+PA), and >15 Venus-negative plaques from each mouse infected with WT-Venus-H5N1 virus (Table 4). These results suggest that the Venus-NS segment of rgMA-Venus-H5N1 virus is more stable than that of WT+MA-(PB2+PA) virus in mice and that viral segments other than PB2 and PA may also contribute to the stability of the Venus-NS segment in MA-Venus-H5N1 virus *in vivo*.

DISCUSSION

Previously, we constructed an H5N1 virus expressing a Venus reporter gene that became more lethal to mice and more stable after mouse adaptation (9). In this study, we sequenced the whole genome of this virus (MA-Venus-H5N1) and identified 7 amino acids that differed from the WT-Venus-H5N1 virus sequence. To explore the molecular determinants of the differences in virulence and Venus expression in mice between these two viruses, we generated a series of reassortants of both viruses by using reverse genetics. We found that the double mutation of PB2 (V25A) and PA (R443K) dramatically enhanced the pathogenicity of WT-Venus-H5N1 in mice. We also found that the V25A mutation in PB2

TABLE 3 Venus stability in Venus-H5N1 reassortants in MDCK cells[a]

Virus	No. of passages in MDCK cells	No. of plaques examined	No. of Venus-negative plaques
WT-Venus-H5N1	2	73	4
	3	111	1
	4	79	0
	5	61	2
rgMA-Venus-H5N1	2	66	0
	3	144	0
	4	73	0
	5	75	0
WT+MA-PB2	5	84	0
WT+MA-PB1	5	126	1
WT+MA-PA	5	104	0
WT+MA-(PB2+PA)	5	123	0
WT+MA-NS	5	199	0
WT+MA-NA	5	73	1
WT+MA-M	5	69	10[b]

[a] Each virus was passaged five times in MDCK cells, as described in Materials and Methods. Venus expression in stocks from different passages was detected in MDCK cells by using fluorescence microscopy. Venus-negative plaques were picked up and amplified in MDCK cells. Amplified Venus-negative plaques were reassessed for Venus expression to exclude false-negative plaques.

[b] Sixty-nine plaques of the fifth-passage stock of WT+MA-M were examined by using fluorescence microscopy, and all of them were "Venus negative." Ten of these plaques were picked up to further confirm the lack of Venus expression, all of which were confirmed to be Venus negative.

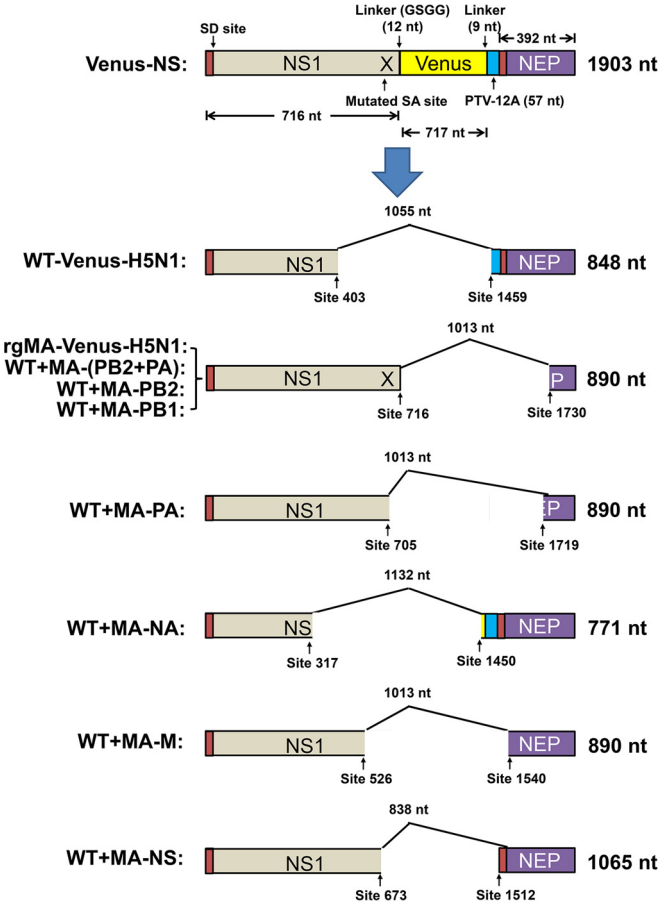

FIG 8 Deletion of Venus-NS segments from Venus-H5N1 reassortants. Viruses were passaged five times in MDCK cells, and the vRNAs from the fifth passages were extracted by using a QIAamp viral RNA minikit (Qiagen). The respective NS segments were then amplified by PCR with NS-specific primers, and the deleted NS segments (shown in Fig. 7) were extracted and sequenced. The deletion types were determined by comparing the sequences of deleted NS and Venus-NS. nt, nucleotides; SD, splice donor; SA, splice acceptor; PTV-12A, porcine teschovirus-1 (PTV-1) 2A autoproteolytic cleavage site.

significantly increased Venus expression and viral replication in MDCK cells and in mice and that the R443K mutation in PA further enhanced these effects. When we examined the Venus stability of the different reassortants *in vitro*, we found that the reassortants with MA-PB2, MA-PA, or MA-NS were more stable. These results suggest that the PB2 and PA proteins play important roles in the pathogenicity and Venus stability of this Venus-expressing H5N1 virus in mammalian hosts.

The pathogenicity of H5N1 HPAIV in mammals is determined by multiple viral genes. For example, the HA protein of HPAIV plays crucial roles in systemic replication and lethal infection in chickens (24) and mammals (25, 26). Mutations in the M1 protein also affect the virulence of H5N1 viruses in mice (27). The amino acids at positions 627 and 701 of PB2 are key determinants of the high virulence of H5N1 influenza viruses in mammals (25, 28). Finally, the PA protein contributes to the virulence of H5N1 avian influenza viruses in domestic ducks (29) and in mice (30). Here, we found that the V25A mutation in PB2 and the R443K mutation in PA synergistically contribute to the pathogenicity of H5N1 virus in mice.

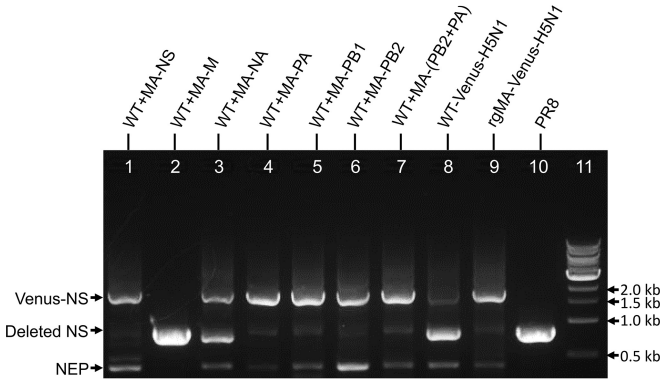

FIG 7 Venus-NS and deleted NS segments of Venus-H5N1-related reassortants. Viruses were passaged five times in MDCK cells, and the vRNAs from the fifth passages were extracted by using a QIAamp viral RNA minikit (Qiagen). The respective NS segments were then amplified by PCR with NS-specific primers and run on an agarose gel. Lane 1, WT+MA-NS; lane 2, WT+MA-M; lane 3, WT+MA-NA; lane 4, WT+MA-PA; lane 5, WT+MA-PB1; lane 6, WT+MA-PB2; lane 7, WT+MA-(PB2+PA); lane 8, WT-Venus-H5N1; lane 9, rgMA-Venus-H5N1; lane 10, PR8; lane 11, 1-kb DNA marker.

Based on all of the influenza virus sequences (23,514 PB2 proteins and 24,240 PA proteins) available in the public database (http://www.fludb.org/), we found that 25V in PB2 and 443R in PA are extremely conserved, whereas 25A in PB2 is present in only two viruses [A/Mallard/ON/499/2005(H5N1) (GenBank accession number EF392844) and A/Zhejiang/92/2009(H1N1) (accession number CY095997)], and 443K in PA is present in only one strain, isolated from a quail [A/Quail/Shantou/1425/2001(H9N2) (accession number EF154846)]. Although the virulence of these

TABLE 4 Venus stability in Venus-H5N1 viruses in mice[a]

Virus	Mouse	No. of plaques examined	No. of Venus-negative plaques
rgMA-Venus-H5N1	1	105	1
	2	109	0
	3	127	0
WT+MA-(PB2+PA)	4	116	6
	5	111	3
	6	115	3
WT-Venus-H5N1	7	145	22
	8	120	18
	9	95	15

[a] Six-week-old C57BL/6 mice were infected intranasally with 10^5 PFU of each virus in a 50-μl volume. Three mice from each group were euthanized on day 4 p.i., and their lung tissues were collected and homogenized in PBS. The supernatants of the lung samples were inoculated into MDCK cells to check for Venus expression, and Venus-negative plaques were picked up and amplified in MDCK cells. Amplified Venus-negative plaques were rechecked for Venus expression to exclude false-negative plaques.

viruses in mice is unknown, our study suggests that the combination of 25A in PB2 and 443K in PA contributes to increased virulence in mice and is a unique feature of MA-Venus-H5N1 virus.

The RNA polymerase of influenza A virus consists of the PB1, PB2, and PA subunits and is implicated in numerous essential processes in the viral life cycle (31). PB1 performs polymerase activities, PB2 is responsible for capped-RNA recognition, and PA is involved in RNA replication and proteolytic activity (32). The interaction of these polymerase subunits is essential for transcription initiation (33, 34). Residues 1 to 37 at the N terminus of the PB2 protein play a vital role in binding to the PB1 protein and affect the RNA polymerase activity; these residues are highly conserved among all subtypes of influenza virus (33). The amino acid at position 25 of PB2 is located within the third α-helix (amino acids 25 to 32) of its PB1-binding domain (33). In this study, we found that that the V25A mutation in PB2 enhances viral replication in mammalian cells and in mice, resulting in higher pathogenicity of the H5N1 virus in mice. The R443 residue of the PA protein also plays an important role in replicative activity (32, 35), and the R443A mutation in PA prevents the production of infectious virus (35). Here, we showed that a virus with PA-443K is viable and demonstrated that the R443K mutation in PA enhances viral replication in mouse lungs. Our data thus further emphasize the important role of the amino acid at position 443 of the PA protein for influenza virus.

Previous studies reported that the polymerase activity of the viral RNP complex closely correlates with viral replication and virulence (20–23). Viruses with higher polymerase activity in mammalian cells generally show higher virulence in mice (36) and ferrets (21). However, H5N1 reassortants containing genes from pandemic H1N1 virus enhanced viral replication in A549 cells but possessed lower polymerase activity than that of the parental H5N1 virus (37). Similarly, reassortants with higher polymerase activity were less pathogenic in mice than were their wild-type counterparts (38, 39). In this study, we found that MA-Venus-H5N1 virus was more lethal to mice than was its wild-type counterpart, yet it had much lower polymerase activity, and any RNP combination with a polymerase gene from MA-Venus-H5N1 also had lower activity. Although our results appear to contradict the results from the previous studies mentioned above, they support previously reported findings that high pathogenicity of a virus requires an optimal, appropriate level of polymerase activity (20). The influenza virus nuclear export protein (NEP) has been shown to play a role in regulating viral polymerase activity, and the NEP/NS1 protein ratio affects viral RNA transcription and translation (40, 41). In the Venus-H5N1 virus, NEP was not produced from a spliced message; rather, a single polyprotein was expressed and then processed into NS1-Venus and NEP. This modification of the NS segment was previously shown to significantly decrease the NEP expression level (42), which may have resulted in the decreased replicative efficiency and attenuation of WT-Venus-H5N1 virus in mice. The PB2 V25A and PA R443K mutations may somehow compensate for this decrease in the NEP expression level.

With the development of live imaging *in vivo*, the ability to visualize influenza viruses carrying fluorescent reporter genes will be of great benefit to influenza virus-related research (6, 7, 9, 43, 44). An effective virus for this purpose should have good replicative ability and show considerable pathogenicity in its host. Moreover, its fluorescent reporter protein should be both highly and stably expressed. Many attempts to construct influenza A viruses carrying the green fluorescent protein (GFP) reporter gene have been reported (7, 45, 46); however, some of these viruses showed a low level of replication or poor pathogenicity in mice (45), whereas others produced relatively low fluorescence signals or did not stably express GFP during virus replication *in vitro* and *in vivo* (7). Our data demonstrate that not only is MA-Venus-H5N1 virus highly pathogenic to mice, it also highly and stably expresses Venus fluorescent protein *in vitro* and *in vivo*. In our analysis of the molecular determinants of Venus expression and Venus stability, we found that the V25A mutation in PB2 played an important role in determining Venus expression, which was further enhanced by the presence of the R443K mutation in PA. Our analysis of Venus stability revealed that the single MA-PB1, -PB2, -PA, or -NS gene determines Venus stability *in vitro*, but *in vivo*, the situation is more complex, and mutations in PB1, PB2, PA, and NS may synergistically codetermine Venus stability in MA-Venus-H5N1 virus. With the development of the multiphoton microscopy technique and fluorophores with long emission at the near-infrared region, *in vivo* fluorescence imaging is advancing. Kreisel et al. (47) and Looney et al. (48) have successfully established *in vivo* imaging of lungs by using multiphoton microscopy with fluorescent proteins. Therefore, MA-Venus-H5N1 virus is a good model virus for *in vivo* imaging studies.

In summary, here we identified the molecular determinants in a mouse-adapted Venus-H5N1 virus that play an important role in the pathogenicity of the virus in mice and in its Venus expression and Venus stability *in vitro* and *in vivo*. These molecular markers will be of value to future influenza virus-related live-imaging research.

ACKNOWLEDGMENTS

We thank Susan Watson for editing the manuscript.

This work was supported by the Japan Initiative for Global Research Network on Infectious Diseases from the Ministry of Education, Culture, Sports, Science and Technology, Japan; by grants-in-aid from the Ministry of Health, Labor and Welfare, Japan; by ERATO and the Strategic Basic Research Programs of the Japan Science and Technology Agency; by the Advanced Research & Development Programs for Medical Innovation

from the Japan Agency for Medical Research and Development (AMED); and by an NIAID-funded Center for Research on Influenza Pathogenesis (CRIP) grant (HHSN266200700010C). H. Katsura is supported by JSPS research fellowships for young scientists.

REFERENCES

1. **Li Z, Jiang Y, Jiao P, Wang A, Zhao F, Tian G, Wang X, Yu K, Bu Z, Chen H.** 2006. The NS1 gene contributes to the virulence of H5N1 avian influenza viruses. J Virol **80:**11115–11123. http://dx.doi.org/10.1128/JVI.00993-06.
2. **Li Y, Shi J, Zhong G, Deng G, Tian G, Ge J, Zeng X, Song J, Zhao D, Liu L, Jiang Y, Guan Y, Bu Z, Chen H.** 2010. Continued evolution of H5N1 influenza viruses in wild birds, domestic poultry, and humans in China from 2004 to 2009. J Virol **84:**8389–8397. http://dx.doi.org/10.1128/JVI.00413-10.
3. **Neumann G, Chen H, Gao GF, Shu Y, Kawaoka Y.** 2010. H5N1 influenza viruses: outbreaks and biological properties. Cell Res **20:**51–61. http://dx.doi.org/10.1038/cr.2009.124.
4. **Chen H, Yuan H, Gao R, Zhang J, Wang D, Xiong Y, Fan G, Yang F, Li X, Zhou J, Zou S, Yang L, Chen T, Dong L, Bo H, Zhao X, Zhang Y, Lan Y, Bai T, Dong J, Li Q, Wang S, Zhang Y, Li H, Gong T, Shi Y, Ni X, Li J, Zhou J, Fan J, Wu J, Zhou X, Hu M, Wan J, Yang W, Li D, Wu G, Feng Z, Gao GF, Wang Y, Jin Q, Liu M, Shu Y.** 2014. Clinical and epidemiological characteristics of a fatal case of avian influenza A H10N8 virus infection: a descriptive study. Lancet **383:**714–721. http://dx.doi.org/10.1016/S0140-6736(14)60111-2.
5. **Li Q, Zhou L, Zhou M, Chen Z, Li F, Wu H, Xiang N, Chen E, Tang F, Wang D, Meng L, Hong Z, Tu W, Cao Y, Li L, Ding F, Liu B, Wang M, Xie R, Gao R, Li X, Bai T, Zou S, He J, Hu J, Xu Y, Chai C, Wang S, Gao Y, Jin L, Zhang Y, Luo H, Yu H, He J, Li Q, Wang X, Gao L, Pang X, Liu G, Yan Y, Yuan H, Shu Y, Yang W, Wang Y, Wu F, Uyeki TM, Feng Z.** 2014. Epidemiology of human infections with avian influenza A(H7N9) virus in China. N Engl J Med **370:**520–532. http://dx.doi.org/10.1056/NEJMoa1304617.
6. **Helft J, Manicassamy B, Guermonprez P, Hashimoto D, Silvin A, Agudo J, Brown BD, Schmolke M, Miller JC, Leboeuf M, Murphy KM, Garcia-Sastre A, Merad M.** 2012. Cross-presenting CD103+ dendritic cells are protected from influenza virus infection. J Clin Invest **122:**4037–4047. http://dx.doi.org/10.1172/JCI60659.
7. **Manicassamy B, Manicassamy S, Belicha-Villanueva A, Pisanelli G, Pulendran B, Garcia-Sastre A.** 2010. Analysis of in vivo dynamics of influenza virus infection in mice using a GFP reporter virus. Proc Natl Acad Sci U S A **107:**11531–11536. http://dx.doi.org/10.1073/pnas.0914994107.
8. **Nagai T, Ibata K, Park ES, Kubota M, Mikoshiba K, Miyawaki A.** 2002. A variant of yellow fluorescent protein with fast and efficient maturation for cell-biological applications. Nat Biotechnol **20:**87–90. http://dx.doi.org/10.1038/nbt0102-87.
9. **Fukuyama S, Katsura H, Zhao D, Ozawa M, Ando T, Shoemaker JE, Ishikawa I, Yamada S, Neumann G, Watanabe S, Kitano H, Kawaoka Y.** 2015. Multi-spectral fluorescent reporter influenza viruses (Color-flu) as powerful tools for in vivo studies. Nat Commun **6:**6600. http://dx.doi.org/10.1038/ncomms7600.
10. **Neumann G, Watanabe T, Ito H, Watanabe S, Goto H, Gao P, Hughes M, Perez DR, Donis R, Hoffmann E, Hobom G, Kawaoka Y.** 1999. Generation of influenza A viruses entirely from cloned cDNAs. Proc Natl Acad Sci U S A **96:**9345–9350. http://dx.doi.org/10.1073/pnas.96.16.9345.
11. **Dias A, Bouvier D, Crepin T, McCarthy AA, Hart DJ, Baudin F, Cusack S, Ruigrok RW.** 2009. The cap-snatching endonuclease of influenza virus polymerase resides in the PA subunit. Nature **458:**914–918. http://dx.doi.org/10.1038/nature07745.
12. **Yamayoshi S, Yamada S, Fukuyama S, Murakami S, Zhao D, Uraki R, Watanabe T, Tomita Y, Macken C, Neumann G, Kawaoka Y.** 2014. Virulence-affecting amino acid changes in the PA protein of H7N9 influenza A viruses. J Virol **88:**3127–3134. http://dx.doi.org/10.1128/JVI.03155-13.
13. **Reed LJ, Muench H.** 1938. A simple method of estimating fifty per cent endpoints. Am J Hyg **27:**493–497.
14. **Ozawa M, Fujii K, Muramoto Y, Yamada S, Yamayoshi S, Takada A, Goto H, Horimoto T, Kawaoka Y.** 2007. Contributions of two nuclear localization signals of influenza A virus nucleoprotein to viral replication. J Virol **81:**30–41. http://dx.doi.org/10.1128/JVI.01434-06.
15. **Murakami S, Horimoto T, Yamada S, Kakugawa S, Goto H, Kawaoka Y.** 2008. Establishment of canine RNA polymerase I-driven reverse genetics for influenza A virus: its application for H5N1 vaccine production. J Virol **82:**1605–1609. http://dx.doi.org/10.1128/JVI.01876-07.
16. **Zhao D, Liang L, Li Y, Liu L, Guan Y, Jiang Y, Chen H.** 2012. Proteomic analysis of the lungs of mice infected with different pathotypes of H5N1 avian influenza viruses. Proteomics **12:**1970–1982. http://dx.doi.org/10.1002/pmic.201100619.
17. **Edgar RC.** 2004. MUSCLE: multiple sequence alignment with high accuracy and high throughput. Nucleic Acids Res **32:**1792–1797. http://dx.doi.org/10.1093/nar/gkh340.
18. **Larkin MA, Blackshields G, Brown NP, Chenna R, McGettigan PA, McWilliam H, Valentin F, Wallace IM, Wilm A, Lopez R, Thompson JD, Gibson TJ, Higgins DG.** 2007. Clustal W and Clustal X version 2.0. Bioinformatics **23:**2947–2948. http://dx.doi.org/10.1093/bioinformatics/btm404.
19. **Schmolke M, Manicassamy B, Pena L, Sutton T, Hai R, Varga ZT, Hale BG, Steel J, Perez DR, Garcia-Sastre A.** 2011. Differential contribution of PB1-F2 to the virulence of highly pathogenic H5N1 influenza A virus in mammalian and avian species. PLoS Pathog **7:**e1002186. http://dx.doi.org/10.1371/journal.ppat.1002186.
20. **Gabriel G, Dauber B, Wolff T, Planz O, Klenk HD, Stech J.** 2005. The viral polymerase mediates adaptation of an avian influenza virus to a mammalian host. Proc Natl Acad Sci U S A **102:**18590–18595. http://dx.doi.org/10.1073/pnas.0507415102.
21. **Salomon R, Franks J, Govorkova EA, Ilyushina NA, Yen HL, Hulse-Post DJ, Humberd J, Trichet M, Rehg JE, Webby RJ, Webster RG, Hoffmann E.** 2006. The polymerase complex genes contribute to the high virulence of the human H5N1 influenza virus isolate A/Vietnam/1203/04. J Exp Med **203:**689–697. http://dx.doi.org/10.1084/jem.20051938.
22. **Li C, Hatta M, Watanabe S, Neumann G, Kawaoka Y.** 2008. Compatibility among polymerase subunit proteins is a restricting factor in reassortment between equine H7N7 and human H3N2 influenza viruses. J Virol **82:**11880–11888. http://dx.doi.org/10.1128/JVI.01445-08.
23. **Leung BW, Chen H, Brownlee GG.** 2010. Correlation between polymerase activity and pathogenicity in two duck H5N1 influenza viruses suggests that the polymerase contributes to pathogenicity. Virology **401:**96–106. http://dx.doi.org/10.1016/j.virol.2010.01.036.
24. **Kawaoka Y, Webster RG.** 1988. Sequence requirements for cleavage activation of influenza virus hemagglutinin expressed in mammalian cells. Proc Natl Acad Sci U S A **85:**324–328. http://dx.doi.org/10.1073/pnas.85.2.324.
25. **Hatta M, Gao P, Halfmann P, Kawaoka Y.** 2001. Molecular basis for high virulence of Hong Kong H5N1 influenza A viruses. Science **293:**1840–1842. http://dx.doi.org/10.1126/science.1062882.
26. **Suguitan AL, Jr, Matsuoka Y, Lau YF, Santos CP, Vogel L, Cheng LI, Orandle M, Subbarao K.** 2012. The multibasic cleavage site of the hemagglutinin of highly pathogenic A/Vietnam/1203/2004 (H5N1) avian influenza virus acts as a virulence factor in a host-specific manner in mammals. J Virol **86:**2706–2714. http://dx.doi.org/10.1128/JVI.05546-11.
27. **Fan S, Deng G, Song J, Tian G, Suo Y, Jiang Y, Guan Y, Bu Z, Kawaoka Y, Chen H.** 2009. Two amino acid residues in the matrix protein M1 contribute to the virulence difference of H5N1 avian influenza viruses in mice. Virology **384:**28–32. http://dx.doi.org/10.1016/j.virol.2008.11.044.
28. **Li Z, Chen H, Jiao P, Deng G, Tian G, Li Y, Hoffmann E, Webster RG, Matsuoka Y, Yu K.** 2005. Molecular basis of replication of duck H5N1 influenza viruses in a mammalian mouse model. J Virol **79:**12058–12064. http://dx.doi.org/10.1128/JVI.79.18.12058-12064.2005.
29. **Song J, Feng H, Xu J, Zhao D, Shi J, Li Y, Deng G, Jiang Y, Li X, Zhu P, Guan Y, Bu Z, Kawaoka Y, Chen H.** 2011. The PA protein directly contributes to the virulence of H5N1 avian influenza viruses in domestic ducks. J Virol **85:**2180–2188. http://dx.doi.org/10.1128/JVI.01975-10.
30. **Hu J, Hu Z, Song Q, Gu M, Liu X, Wang X, Hu S, Chen C, Liu H, Liu W, Chen S, Peng D, Liu X.** 2013. The PA-gene-mediated lethal dissemination and excessive innate immune response contribute to the high virulence of H5N1 avian influenza virus in mice. J Virol **87:**2660–2672. http://dx.doi.org/10.1128/JVI.02891-12.
31. **Naffakh N, Tomoiu A, Rameix-Welti MA, van der Werf S.** 2008. Host restriction of avian influenza viruses at the level of the ribonucleoproteins. Annu Rev Microbiol **62:**403–424. http://dx.doi.org/10.1146/annurev.micro.62.081307.162746.
32. **Obayashi E, Yoshida H, Kawai F, Shibayama N, Kawaguchi A, Nagata K, Tame JR, Park SY.** 2008. The structural basis for an essential subunit

interaction in influenza virus RNA polymerase. Nature **454:**1127–1131. http://dx.doi.org/10.1038/nature07225.
33. **Sugiyama K, Obayashi E, Kawaguchi A, Suzuki Y, Tame JR, Nagata K, Park SY.** 2009. Structural insight into the essential PB1-PB2 subunit contact of the influenza virus RNA polymerase. EMBO J **28:**1803–1811. http://dx.doi.org/10.1038/emboj.2009.138.
34. **He X, Zhou J, Bartlam M, Zhang R, Ma J, Lou Z, Li X, Li J, Joachimiak A, Zeng Z, Ge R, Rao Z, Liu Y.** 2008. Crystal structure of the polymerase PA(C)-PB1(N) complex from an avian influenza H5N1 virus. Nature **454:** 1123–1126. http://dx.doi.org/10.1038/nature07120.
35. **Regan JF, Liang Y, Parslow TG.** 2006. Defective assembly of influenza A virus due to a mutation in the polymerase subunit PA. J Virol **80:**252–261. http://dx.doi.org/10.1128/JVI.80.1.252-261.2006.
36. **Zhang H, Li X, Guo J, Li L, Chang C, Li Y, Bian C, Xu K, Chen H, Sun B.** 2014. The PB2 E627K mutation contributes to the high polymerase activity and enhanced replication of H7N9 influenza virus. J Gen Virol **95:**779–786. http://dx.doi.org/10.1099/vir.0.061721-0.
37. **Octaviani CP, Ozawa M, Yamada S, Goto H, Kawaoka Y.** 2010. High level of genetic compatibility between swine-origin H1N1 and highly pathogenic avian H5N1 influenza viruses. J Virol **84:**10918–10922. http://dx.doi.org/10.1128/JVI.01140-10.
38. **Zhang Y, Zhang Q, Kong H, Jiang Y, Gao Y, Deng G, Shi J, Tian G, Liu L, Liu J, Guan Y, Bu Z, Chen H.** 2013. H5N1 hybrid viruses bearing 2009/H1N1 virus genes transmit in guinea pigs by respiratory droplet. Science **340:**1459–1463. http://dx.doi.org/10.1126/science.1229455.
39. **Sun Y, Qin K, Wang J, Pu J, Tang Q, Hu Y, Bi Y, Zhao X, Yang H, Shu Y, Liu J.** 2011. High genetic compatibility and increased pathogenicity of reassortants derived from avian H9N2 and pandemic H1N1/2009 influenza viruses. Proc Natl Acad Sci U S A **108:**4164–4169. http://dx.doi.org/10.1073/pnas.1019109108.
40. **Robb NC, Smith M, Vreede FT, Fodor E.** 2009. NS2/NEP protein regulates transcription and replication of the influenza virus RNA genome. J Gen Virol **90:**1398–1407. http://dx.doi.org/10.1099/vir.0.009639-0.
41. **Fournier G, Chiang C, Munier S, Tomoiu A, Demeret C, Vidalain PO, Jacob Y, Naffakh N.** 2014. Recruitment of RED-SMU1 complex by influenza A virus RNA polymerase to control viral mRNA splicing. PLoS Pathog **10:**e1004164. http://dx.doi.org/10.1371/journal.ppat.1004164.
42. **Chua MA, Schmid S, Perez JT, Langlois RA, Tenoever BR.** 2013. Influenza A virus utilizes suboptimal splicing to coordinate the timing of infection. Cell Rep **3:**23–29. http://dx.doi.org/10.1016/j.celrep.2012.12.010.
43. **Heaton NS, Leyva-Grado VH, Tan GS, Eggink D, Hai R, Palese P.** 2013. In vivo bioluminescent imaging of influenza A virus infection and characterization of novel cross-protective monoclonal antibodies. J Virol **87:** 8272–8281. http://dx.doi.org/10.1128/JVI.00969-13.
44. **Pan W, Dong Z, Li F, Meng W, Feng L, Niu X, Li C, Luo Q, Li Z, Sun C, Chen L.** 2013. Visualizing influenza virus infection in living mice. Nat Commun **4:**2369. http://dx.doi.org/10.1038/ncomms3369.
45. **Kittel C, Sereinig S, Ferko B, Stasakova J, Romanova J, Wolkerstorfer A, Katinger H, Egorov A.** 2004. Rescue of influenza virus expressing GFP from the NS1 reading frame. Virology **324:**67–73. http://dx.doi.org/10.1016/j.virol.2004.03.035.
46. **Shinya K, Fujii Y, Ito H, Ito T, Kawaoka Y.** 2004. Characterization of a neuraminidase-deficient influenza A virus as a potential gene delivery vector and a live vaccine. J Virol **78:**3083–3088. http://dx.doi.org/10.1128/JVI.78.6.3083-3088.2004.
47. **Kreisel D, Nava RG, Li W, Zinselmeyer BH, Wang B, Lai J, Pless R, Gelman AE, Krupnick AS, Miller MJ.** 2010. In vivo two-photon imaging reveals monocyte-dependent neutrophil extravasation during pulmonary inflammation. Proc Natl Acad Sci U S A **107:**18073–18078. http://dx.doi.org/10.1073/pnas.1008737107.
48. **Looney MR, Thornton EE, Sen D, Lamm WJ, Glenny RW, Krummel MF.** 2011. Stabilized imaging of immune surveillance in the mouse lung. Nat Methods **8:**91–96. http://dx.doi.org/10.1038/nmeth.1543.
49. **Holm S.** 1979. A simple sequentially rejective multiple test procedure. Scand J Stat **6:**65–70.